Relative contributions of heat flux and wind stress on the spatiotemporal upper-ocean variability in the tropical Indian Ocean

Environmental Research Letters

LETTER

Relative contributions of heat flux and wind stress on the spatiotemporal upper-ocean variability in the tropical Indian Ocean

Xu Yuan[1], Caroline C Ummenhofer[2], Hyodae Seo[2] and Zhongbo Su[1]

[1] Faculty of Geo-Information Science and Earth Observation (ITC), University of Twente, The Netherlands
[2] Department of Physical Oceanography, Woods Hole Oceanographic Institution, Woods Hole, Massachusetts, United States of America

E-mail: x.yuan@utwente.nl

Keywords: interannual variability, tropical Indian Ocean, heat flux, wind stress, subsurface temperature

Supplementary material for this article is available online

OPEN ACCESS

RECEIVED
13 December 2019

REVISED
16 June 2020

ACCEPTED FOR PUBLICATION
23 June 2020

PUBLISHED
12 August 2020

Abstract

High-resolution ocean general circulation model (OGCM) simulations are employed to investigate interannual variability of the upper-ocean temperature in the tropical Indian Ocean (20°S–20°N). The seasonal cycle and interannual variability in the upper-ocean temperature in the tropical Indian Ocean in the forced ocean simulation are in good agreement with available observation and reanalysis products. Two further sensitivity OGCM simulations are used to separate the relative contributions of heat flux and wind stress. The comparison of the model simulations reveals the depth-dependent influences of heat flux and wind stress on the ocean temperature variability in the tropical Indian Ocean. Generally, heat flux dominates the temperature variability in the top 30 m, while wind stress contributes most strongly to the subsurface temperature variability below 30 m. This implies that a transition depth should exist at each location, where the dominant control of the ocean temperature variability switched from heat flux to wind stress. We define the depth of this transition point as the 'crossing depth' and make use of this concept to better understand the depth-dependent impacts of the heat flux and wind stress on the upper-ocean temperature variability in the tropical Indian Ocean. The crossing depth tends to be shallower in the southern tropical Indian Ocean (20°S-EQ), including the Seychelles-Chagos Thermocline Ridge (SCTR) and the eastern part of the Indian Ocean Dipole (IOD), suggesting the dominance of forcing due to wind stress and the resulting ocean dynamical processes in the temperature variability in those regions. The crossing depth also shows prominent seasonal variability in the southern tropical Indian Ocean. In the SCTR, the variability of the subsurface temperature forced by the wind stress dominates largely in boreal winter and spring, resulting in the shallow crossing depth in these seasons. In contrast, the intensified subsurface temperature variability with shallow crossing depth in the eastern part of the IOD is seen during boreal autumn. Overall, our results suggest that the two regions within the tropical Indian Ocean, the SCTR and the eastern part of the IOD, are the primary locations where the ocean dynamics due to wind-stress forcing control the upper-ocean temperature variability.

1. Introduction

Prominent warming has been observed throughout the global upper-ocean since the 1950 s (Levitus *et al* 2009, 2012). Yet, the rate of warming in the tropical Indian Ocean far exceeds that in the tropical Pacific and Atlantic Oceans (Han *et al* 2014). Existing studies indicate that atmospheric circulation patterns are closely related to the upper-ocean temperature and sea surface temperature (SST) variability in the tropical Indian Ocean (e.g. Ashok *et al* 2004, Annamalai *et al* 2005, Trenary and Han 2012).

In the tropical oceans, net heat flux and wind stress are the main drivers of the variability in SST and subsurface ocean temperature on seasonal to interannual timescales (e.g. Behera *et al* 2000, Rao

and Sivakumar 2000, Schott *et al* 2009, Sayantani and Gnanaseelan 2015). The net heat flux, consisting of short and long-wave radiative fluxes and the latent and sensible heat fluxes, is the key term in the upper-ocean temperature equation (Moisan and Niiler 1998). Not only is the net heat flux the main driver for seasonal variability of upper-ocean temperature in most areas of the tropical Indian Ocean (Rao and Sivakumar 2000, Cyriac *et al* 2019), but it also plays a vital role in controlling interannual SST variations associated with the El Niño-Southern Oscillation (ENSO) (Behera *et al* 2000). In particular, heat flux into the ocean in the tropical Indian Ocean is shown to be enhanced during the El Niño years in association with the induced atmospheric circulation changes (i.e. atmospheric bridge) (Klein *et al* 1999, Alexander *et al* 2002, Lau and Nath 2003, Liu and Alexander 2007), often inducing basin-wide warming during boreal winter (Shinoda *et al* 2004a, Zhong *et al* 2005).

Behera *et al* (2000) pointed out that the interannual variability of upper-ocean temperature within the Seychelles-Chagos Thermocline Ridge (SCTR) region in the southwestern tropical Indian Ocean, cannot be fully explained by heat flux alone. The SCTR is unique in that the thermocline depth remains climatologically shallow (Schott *et al* 2009). As a result, a strong coupling between the surface and subsurface temperature fields is observed in the SCTR, enabling interannual variability of SST to be sensitive to the subsurface temperature variability driven by local and remote wind stress forcing (Xie *et al* 2002). Du *et al* (2009) suggested that interannual variability of SST in the SCTR is influenced by ocean dynamics within the tropical Indian Ocean and the Rossby wave forced by ENSO (Yamagata *et al* 2004, Yu *et al* 2005, Zhou *et al* 2008). During El Niño years, SST warming in the SCTR is due to a thickened thermocline depth induced by the downwelling Rossby waves in boreal winter and spring (Xie *et al* 2002). In contrast, during La Nina years, SST cooling is related to the upwelling Rossby wave in boreal winter (Singh *et al* 2013).

Moreover, the interannual variability of SST in the eastern tropical Indian Ocean also cannot be solely explained by heat flux variation. Murtugudde and Busalacchi (1999) suggested that wind stress is an indispensable contributor to interannual warming in some regions within the tropical Indian Ocean, such as the Arabian Sea and the southern tropical Indian Ocean. In fact, the well-known Indian Ocean Dipole (IOD) mode arises from enhanced southeasterly monsoon winds along Java and Sumatra, resulting in pronounced interannual SST variability in the tropical Indian Ocean through the Bjerknes feedback (Saji *et al* 1999). For instance, during the positive IOD years co-occurring with ENSO, the surface cooling in the eastern tropical Indian Ocean results from the negative heat flux anomaly (Tanizaki *et al* 2017). However, during the IOD years independent of ENSO, the cooling is a response to wind-driven upwelling during boreal summer-autumn (Chen *et al* 2016, Delman *et al* 2016).

Despite the apparent simultaneous effects of heat flux and wind stress, their relative contribution to interannual variability of upper-ocean temperature in the tropical Indian Ocean has not been systematically quantified. Here, we use a series of high-resolution ocean general circulation model (OGCM) simulations to investigate the relative impacts of heat flux and wind stress on the upper-ocean temperature interannual variability in the tropical Indian Ocean, focusing on their spatial distribution, vertical structure, and seasonal variability. In this exploration, we will use the concept of a 'crossing depth' to tease apart and diagnose the relative contributions of buoyancy and wind stress forcing.

The remainder of the paper is structured as follows. In section 2, we introduce the OGCM and analysis methods. Section 3 details the relative contribution of buoyancy and wind stress forcing to the variability of the tropical Indian Ocean. In section 4, we provide a brief summary and discussion for our findings.

2. Data and methods

2.1. Ocean model simulations

Numerical experiments were performed with the Nucleus for European Modelling of the Ocean (NEMO, version 3.1.1; Madec 2008). We used an eddy-active global ocean-sea ice configuration with a spatial resolution of 0.25° latitude/longitude, ORCA025. The ocean model is coupled to a dynamic-thermodynamic sea-ice model, namely the Louvain-La-Neuve sea-ice Model version 2 (LIM2; Fichefet and Maqueda 1997). The model uses a tripolar grid that has a 21–28 km effective resolution in the tropical Indian Ocean. Its vertical coordinate is discretized with 46 height (z) levels, ranging from 6 m at the surface to 250 m for bottom layers. The lowest grid cells apply a partial step topography (Bernard *et al* 2006). The model has 15 layers in the top 250 m of relevance to the study here. However, it is noteworthy that the results could be dependent on the exact vertical structure compared to another ORCA configuration with 75 vertical levels. Vertical mixing and boundary layer mixing are parameterized by a turbulent kinetic energy scheme (Blanke and Delecluse 1993). Lateral diffusion is performed along isopycnal surfaces.

The initial conditions of the model for temperature and salinity are obtained from climatology (Levitus *et al* 1998). A 30-yr spin-up was forced with interannually varying atmospheric forcing over the period 1978–2007, followed by a series of OGCM simulations that cover the period 1948–2007. The first four years (1948–1951) of the OGCM simulations might still contain adjustment to the initial spin-up period

and thus are excluded from the subsequent analysis. The atmospheric forcing fields are adapted from the corrected global observational dataset based on the National Centers for Environmental Prediction (NCEP)-National Center for Atmospheric Research (NCAR) reanalysis products (Large and Yeager 2009). Specifically, atmospheric variables include 6-hourly wind, air temperature, and humidity; daily shortwave and longwave radiation; monthly precipitation and runoff. In addition to the interannually varying atmospheric forcing, the simulations also make use of the Coordinated Ocean Reference Experiments 2 (CORE2; Griffies *et al* 2009) 'normal year' forcing that is representative of a climatological year but still includes realistic synoptic variability.

Specifically, we use three simulations and analyze output for the period 1952–2007 to examine the role of wind stress and heat flux on interannual variability of upper-ocean temperature in the tropical Indian Ocean. The reference run is forced with full interannual forcing in both heat flux and wind stress and will be hereafter referred to as ALL. The second run is forced with interannually varying heat flux, but with wind stress from the 'normal year' forcing (i.e. climatology), thereby lacking interannual variability in the wind stress field. This simulation is henceforth called HF. Conversely, the third experiment is integrated with interannually varying wind stress at the surface, while heat flux is from the 'normal year' forcing. This simulation is henceforth called WS. To be able to correct for any remaining spurious model drift, a fourth simulation had been conducted forced with the 'normal year' forcing in both the heat flux and wind stress. Linear trends from this 'normal year' simulation for the period 1952–2007 were then used to remove that component of the linear trends in all three simulations (ALL, HF, and WS) that is due to spurious model drift (rather than trends inherent in the forcing fields). However, it should be noted that these linear trends in upper ocean temperatures in the 'normal year' simulation are very small (See more details in Ummenhofer *et al* 2013, 2017).

There are a few caveats in our experimental set-up to note before proceeding. First, the experiments are based on an OGCM forced by atmospheric fields, and thus the set-up does not allow for feedback from the ocean to the atmosphere. More importantly, the heat fluxes in the simulations are calculated through bulk formulae using the prescribed surface air temperature/humidity and the simulated SST. This means that even in the WS run, where wind stress is the only forcing that varies interannually, actual heat flux can vary as it reflects the SST response to interannual wind stress forcing. However, since the use of bulk formula represents essentially a restoring of simulated SST toward the prescribed air-temperature on time scales of a month, this unwanted effect might be considered small. Details for the model configuration can be found in Behrens *et al* (2013). Comparable ORCA simulations at both 0.5° and 0.25° horizontal resolution were employed previously to study Indian Ocean variability on seasonal, interannual, to multi-decadal time scale and were found to adequately reproduce the upper-ocean thermal structure of the Indian Ocean (Schwarzkopf and Böning 2011, Ummenhofer *et al* 2013, 2017, Jin *et al* 2018).

A more detailed comparison between the model and observations can be found in the supplementary material (available online at stacks.iop.org/ERL/15/084047/mmedia).

2.2. Methods

To investigate the spatiotemporal upper-ocean temperature variability of the tropical Indian Ocean, a concept of 'crossing depth' is introduced. We define it based on the standard deviation of interannual ocean temperature obtained from the three model outputs such that,

$$Z_{crossing} = Z_{argmin(Var(T_{HF}(z) - T_{WS}(z)))}$$

where $Z_{crossing}$ is the crossing depth and $Z_{argmin(Var(T_{HF}(z)-T_{WS}(z)))}$ indicates the depth at which the difference of interannual standard deviation between T_{HF} and T_{WS} reaches the minimum. T_{HF} and T_{WS} represent the oceanic temperature, forced by heat flux and wind stress alone, respectively. z represents the oceanic depth.

Monthly mean fields are averaged over different three-month periods for different seasons, such as December-January-February (DJF) for boreal winter, March-April-May (MAM) for boreal spring, June-July-August (JJA) for boreal summer and September-October-November (SON) for boreal autumn, the choice based on the wind changes of the South Asian monsoon and the seasonal change of heat flux (Yu *et al* 2007, Schott *et al* 2009). We confirm that the use of different combinations of months to define seasons, e.g. according to the seasonal variability of upper-ocean temperature variability or thermocline depth produces negligible impacts on our results (figures not shown). The thermocline depth is defined as the depth of the 20 °C isotherms. Mixed layer depth (MLD) is defined as the depth of the water with differences in potential density of less than 0.01 kg m^{-3} relative to the surface.

3. Results

3.1. Depth-dependent effect of heat flux and wind stress forcing on the interannual variability of the upper-ocean temperature fields

Previous studies have shown that interannual variability of the upper-ocean temperature in the tropical Indian Ocean features a significant seasonal phase-locking related to ENSO and IOD (e.g. Behera *et al* 2000, Huang and Kinter 2002). Thus, we compare the seasonal averages of interannual variability of ocean

temperature in the top 180 m averaged over 20°S–20°N, 50°E–100°E (the whole tropical Indian Ocean) from ALL, HF, and WS. In all four seasons, the interannual variability of the whole tropical Indian Ocean from ALL (figures 1(a), (d), (g), (j)) is similar to that of HF (figures 1(b), (e), (h), (k)) in the top 30 m, while its variability is greatly reduced at increasing depth. On the other hand, WS underestimates the variability seen in ALL in the surface layer, only to become comparable to ALL in the deeper ocean. This highlights the depth-dependent role of wind stress and heat flux forcing in determining interannual variability of upper-ocean temperature in the tropical Indian Ocean. Taking the 28 °C isotherm as an example to demonstrate the response to the near-surface temperature, HF well captures the cold and warm events shown in ALL during all seasons, suggesting the year-round effect of heat flux on interannual variability of ocean temperature above the depth of the 28 °C isotherm. On the other hand, the interannual variability of ocean temperature below approximately 28 °C in WS is in good agreement with that in ALL for the four seasons, as shown by the thermocline depth (red line). Thus, the relative impact of heat flux and wind stress on interannual variability of upper-ocean temperature in the tropical Indian Ocean is depth-dependent, and this depth-dependent feature can be found throughout different seasons of the year.

To further quantify the contributions of heat flux and wind stress to the ocean temperature variability, the spatial distributions of the standard deviation of SST and thermocline depth obtained from three simulations are shown in figure 2. The largest values of SST standard deviation near 30°S, consistent with previous work obtained from SST observational data (Baquero-Bernal *et al* 2002), can be seen in all three simulations (figures 2(a), (b)). While the SST standard deviation near the equatorial tropical Indian Ocean (5°S–5°N, 70°E–90°E) in WS is relatively weaker compared to ALL and HF. At depth, in contrast, the standard deviations of thermocline depth in both ALL and WS indicate strong thermocline variability in the southwestern tropical Indian Ocean (5°S–15°S, 50°E–70°E) (figures 2(e), (f)), while the HF run fails to reproduce this thermocline signal.

We also calculate the probability distribution functions of the interannual variability of SST and thermocline depth within the tropical Indian Ocean to further illustrate the relative contributions of heat flux and wind stress on the interannual variability in the tropical Indian Ocean (figures 2(d), (h)). All three experiments exhibit a similar unimodal pattern of SST variability distribution in the tropical Indian Ocean. However, a closer examination shows that the SST variability distribution in WS is displaced towards smaller values by about 0.2 °C compared to that in ALL in the entire tropical Indian Ocean. On the other hand, the distribution of the SST variability in HF is nearly identical to that of ALL. This indicates that heat flux exerts a stronger control on the interannual SST variability in the tropical Indian Ocean. As for the thermocline depth, in contrast, wind stress is the main driver since the thermocline depth variability in both ALL and WS features the bimodal distribution in the tropical Indian Ocean, which is in stark contrast to a unimodal distribution seen in HF. From this analysis, we deduce clear that the influence of heat flux and wind stress on the upper-ocean temperature variability in the whole tropical Indian Ocean is distinct with depth and potentially separable.

We also compare the depth-time diagrams of the ocean temperature from ALL, HF, and WS within the tropical Indian Ocean (20°S-20°N) in figure 3. Again, taking the 28 °C isotherm (thick black line) as an example, HF captures the two cold events in the 1950 s and 1970 s when the isotherm above the 28 °C isotherm outcrops, while WS fails to reproduce such strong events in the tropical Indian Ocean. However, the variability of ocean temperature from WS is almost identical to ALL below the 28 °C isotherm, indicating that the wind stress is the main driver of the interannual temperature variability at the subsurface. This finding is consistent with previous studies showing that interannual variability of the thermocline depth (20 °C; thick red line in figure 3) was found to be entirely attributed to wind stress (Rao and Behera 2005, Yu *et al* 2005). The pronounced spatial differences between SST and thermocline standard deviations in figure 2 also motivate us to examine the depth-dependent influence of heat flux and wind stress in sub-areas of the tropical Indian Ocean, including the SCTR (12°S–5°S, 50°E–75°E), the western tropical Indian Ocean (5°S–5°N, 50°E–75°E), and the eastern tropical Indian Ocean (10°S–5°N, 80°E–100°E). In the SCTR (figures 3(d)–(f)), interannual variability of ocean temperature above the 28 °C isotherm in ALL is better reproduced by HF, while the stronger interannual variability of the subsurface temperature is in good agreement between ALL and WS. In the western tropical Indian Ocean (figures 3(g)–(i)) and eastern tropical Indian Ocean (figure 3(j)–(l)), although the impact of heat flux on interannual variability of ocean temperature does not reach below the depth of the 28 °C isotherm, the simulated temperature between HF and ALL is reasonably consistent in the top 30 m. The interannual variability of ocean temperature below the depth of 28 °C isotherm in WS is consistent with that in ALL. Although there are different physical mechanisms between the northern (EQ-20°N, 50°E–100°E) and the southern (20°S-EQ, 50°E–100°E) tropical Indian Ocean, for example, there is a meridional SST gradient between north and south tropical Indian Ocean due to different wind direction induced by both ENSO and IOD (Wu *et al* 2008), the depth-dependent feature can also be seen in these two areas (figures not shown). Thus, this depth-dependent feature of the impact of heat flux and wind stress on

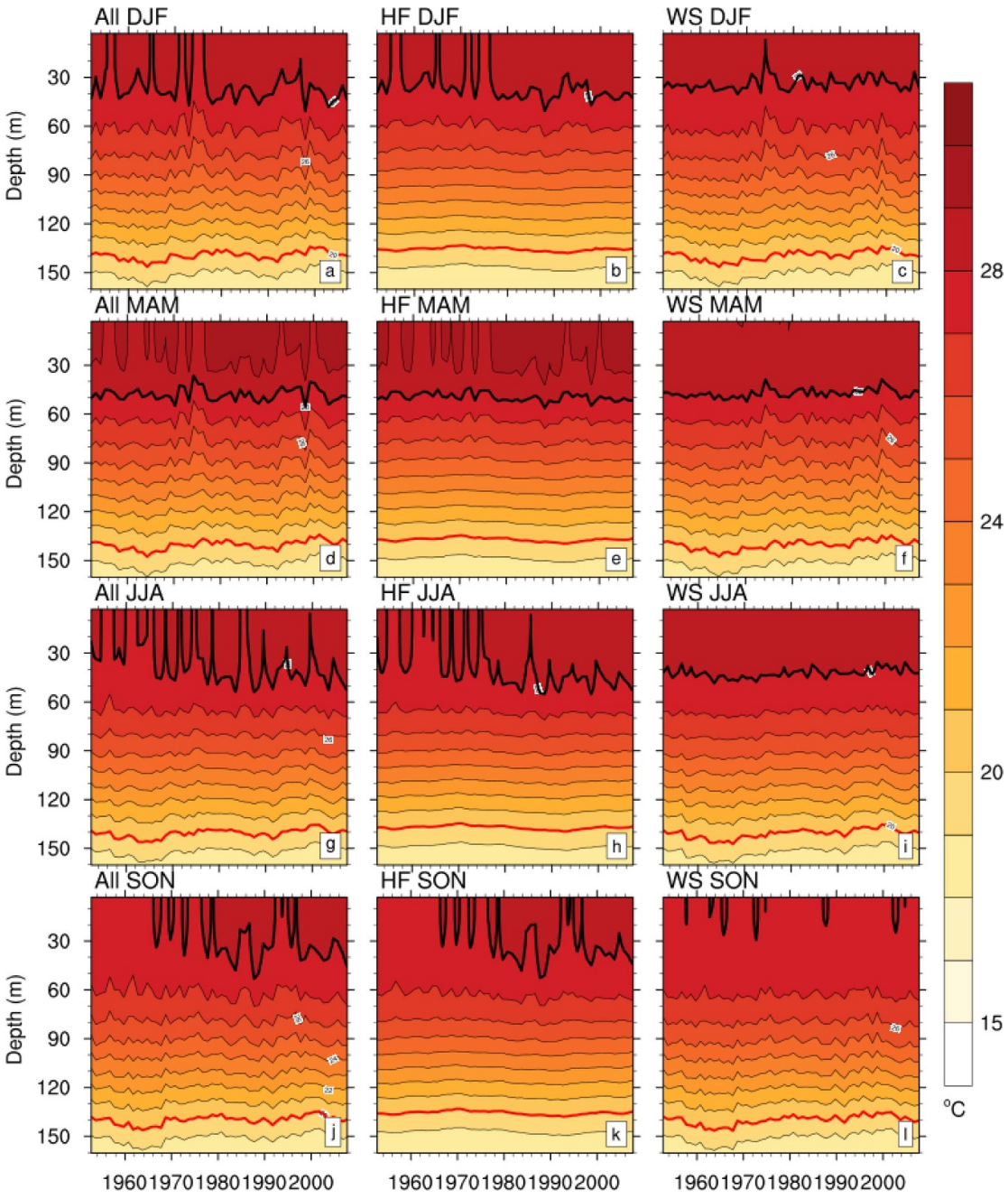

Figure 1. The seasonal upper-ocean temperature in the top 180 m spatially averaged over the area of the tropical Indian Ocean (20°S–20°N, 50°E–100°E) versus depth in the OGCM simulations for ALL, HF, and WS, from 1952 to 2007 during December-January-February (DJF), March-April-May (MAM), June-July-August (JJA) and September-October-November (SON). Unit: °C. The thick black and red lines are the 28 °C and 20 °C isotherms, respectively.

the interannual variability of upper-ocean temperature exists across wide areas in the tropical Indian Ocean.

These depth-dependent influences of heat flux and wind stress are further illustrated in the vertical profiles of the standard deviation of interannual ocean temperature averaged along 50°E–100°E as a function of latitude (figure 4). The consistency of the ocean temperature variability between HF and ALL can only be identified in the top 30 m, which confirms that the effect of heat flux on the ocean temperature variability is limited to the near-surface. In contrast, the comparable ocean temperature variability between WS and ALL is observed in the deeper ocean, indicating that the impact of wind stress is crucial to the subsurface temperature variability. Particularly, WS accurately captures the observed level of the subsurface temperature variability in the SCTR within 4°S–12°S (Vialard *et al* 2009).

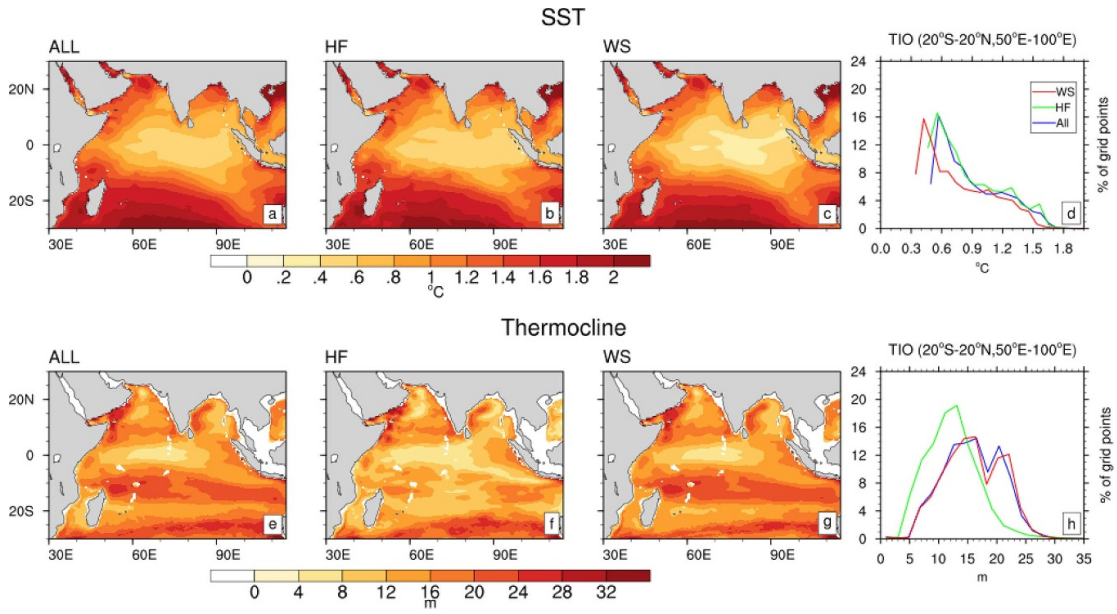

Figure 2. Spatial distributions of the standard deviations of interannual (a)–(c) SST (°C) and (e)–(g) thermocline [m] obtained from three sets of model simulations and their corresponding probability distribution functions (PDF) within the tropical Indian Ocean (20°S–20°N, 50°E–100°E). In the histogram of (d) SST and (h) thermocline, blue, green, and red curves represent ALL, HF, and WS, respectively.

3.2. Crossing depths: attribution of the interannual temperature variability in the tropical Indian Ocean

Such a depth-dependent effect of surface forcing implies that a transition depth would exist, demarcating the regime of heat flux controlled temperature variability near the surface from the deeper depth ranges where the forcing due to wind stress dominates the temperature variability.

Figure 5 shows the distribution of the crossing depth in the tropical Indian Ocean. The shallower crossing depths are located in the southern tropical Indian Ocean associated with a shallower thermocline depth, which is consistent with previous studies (Yokoi *et al* 2008, Schott *et al* 2009). In other words, in the southern equatorial tropical Indian Ocean, heat flux dominates interannual variability of upper-ocean temperature only near the surface, while wind stress plays a more important role at the deeper depth. In the northern tropical Indian Ocean, the crossing depths are deeper than they are in the southern equatorial tropical Indian Ocean, indicating that both heat flux and wind stress contribute to interannual variability of upper-ocean temperature.

However, the crossing depth becomes very deep south of 15°S, where the wind stress impacts both the SST through wind-driven vertical mixing (Behera and Yamagata 2001). We note that the concept of a crossing depth is meaningful only in regions where the effects of wind stress and heat flux can be quasi-linearly separable such as in the tropics and where the thermocline remains relatively shallow. We expect that it does not offer particularly useful information in regions where wind stress also drives significant irreversible mixing that affects the upper ocean temperature fields, such as a layer as in the higher latitudes. Thus, we focus our analysis based on the crossing-depth in two tropical regions, the SCTR and the eastern part of the IOD. These two regions are interesting because SCTR has the shallowest crossing depth, and the eastern part of the IOD supports the most significant interannual ocean temperature variability in the tropical Indian Ocean (Qu and Meyers 2005, Chen *et al* 2016).

Figure 5(b) presents the annual cycle of the crossing depth in the SCTR and eastern part of the IOD. The crossing depth in the SCTR has a clear annual cycle, with the maximum in September at 58 m and a minimum of 23 m in March. This seasonal variation is very similar to the seasonal cycle of SST in the SCTR (Yuan *et al* 2018). From March to August, the crossing depth deepens in the SCTR. The shoaling time of the crossing depth in the SCTR starting from September is in good agreement with the seasonal phase locking impact of ENSO on the SCTR when the SST variability in the SCTR is affected by the ENSO induced anomalous heat flux (Shinoda *et al* 2004b, Nagura and Konda 2007, Burns and Subrahmanyam 2016). The seasonal variability of the crossing depth in the SCTR seems one month lagging than those of MLD. For example, the deepest MLD is in August, while the deepest crossing depth exists in September. The reason is that MLD is defined locally as functions of stratification and vertical shear, which is determined with the local conditions. When the heat flux is cooling or wind stress is strong, it deepens immediately. The crossing depth gets deeper but slowly in the SCTR due to the ocean dynamics (e.g.

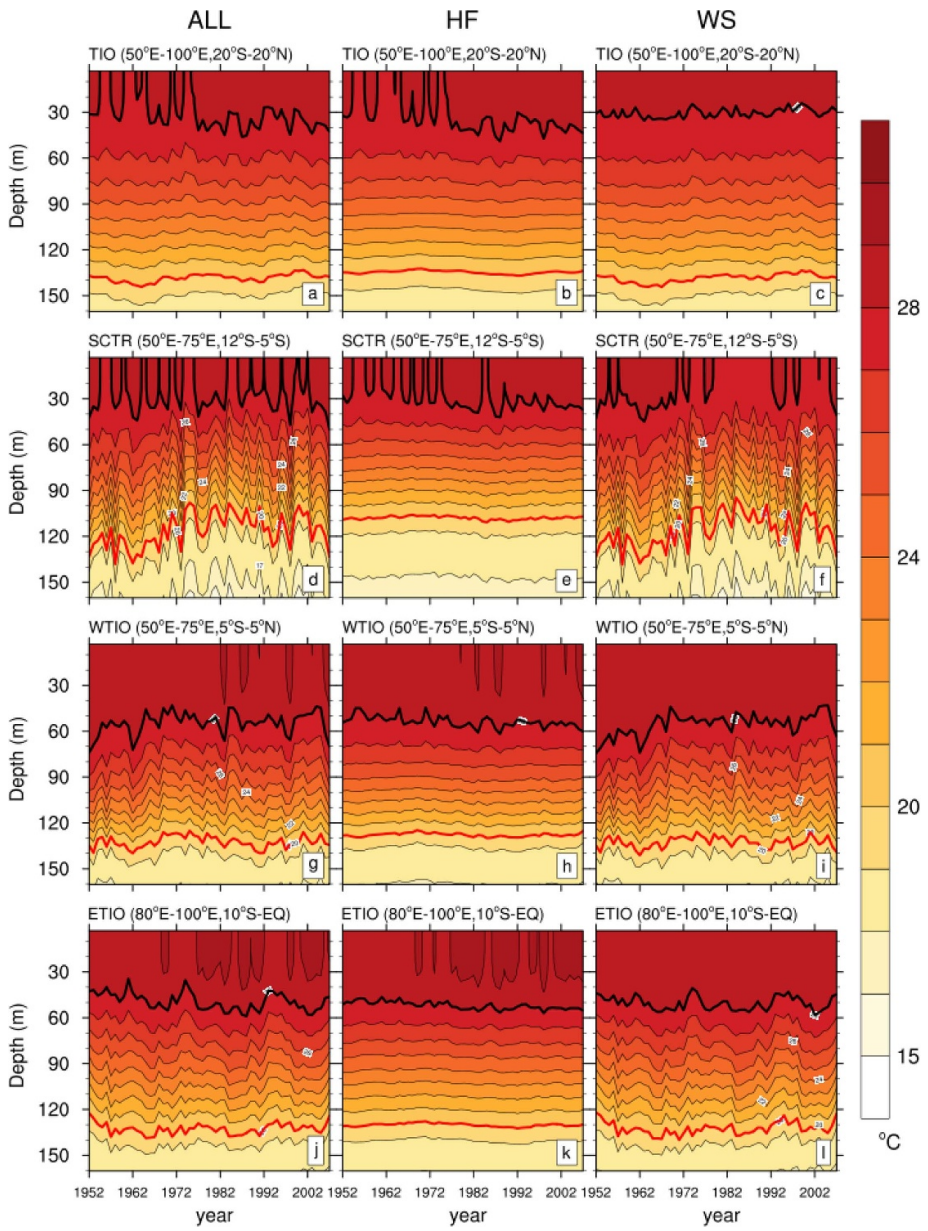

Figure 3. The annual upper-ocean temperature in the top 180 m spatially averaged over the areas of the tropical Indian Ocean (20°S–20°N, 50°E–100°E), SCTR (12°S–5°S, 50°E–75°E), the western tropical Indian Ocean (WTIO, 5°S–5°N, 50°E–75°E) and eastern tropical Indian Ocean (ETIO, 10°S-EQ, 80°E–100°E) versus depth in the OGCM simulations for ALL, HF, and WS, from 1952 to 2007. Unit: °C. The thick black and red lines are the 28 °C and 20 °C isotherms, respectively.

the downwelling Rossby waves). In contrast, the seasonal variation of the crossing depth in the eastern part of the IOD is relatively small, ranging between 30 m and 48 m.

An alternative way to examine the seasonal variability of the crossing depth would be to compare seasonally averaged vertical profiles of the standard deviations of interannual ocean temperature spatially averaged over the SCTR and the eastern part of the IOD (figures 5(c)–(j)). In the SCTR, the depth of the crossing point between HF and WS is in the top 30 m of the water column during boreal winter and spring while it drops to below 30 m during boreal summer and autumn. In the eastern part of the IOD, the transition depth is below 30 m during boreal winter, spring and summer but rises to above 30 m in autumn. Furthermore, corresponding to the shallower crossing depth in boreal winter and spring, interannual variability of the subsurface temperature affected by wind stress is prominent within the SCTR with its standard deviations exceeding 2 °C (figures 5(c), (d)). Similarly, the large interannual variability of the subsurface in the eastern part of the IOD is seen along with the shallower crossing depth in boreal winter and autumn, but its magnitude is weaker (1.5 °C standard deviation, figures 5(i), (j)). Therefore, the crossing depth can separate the relative role of heat flux from wind stress in ocean temperature variability, as well as potentially be an indicator of the intensity of the subsurface variability.

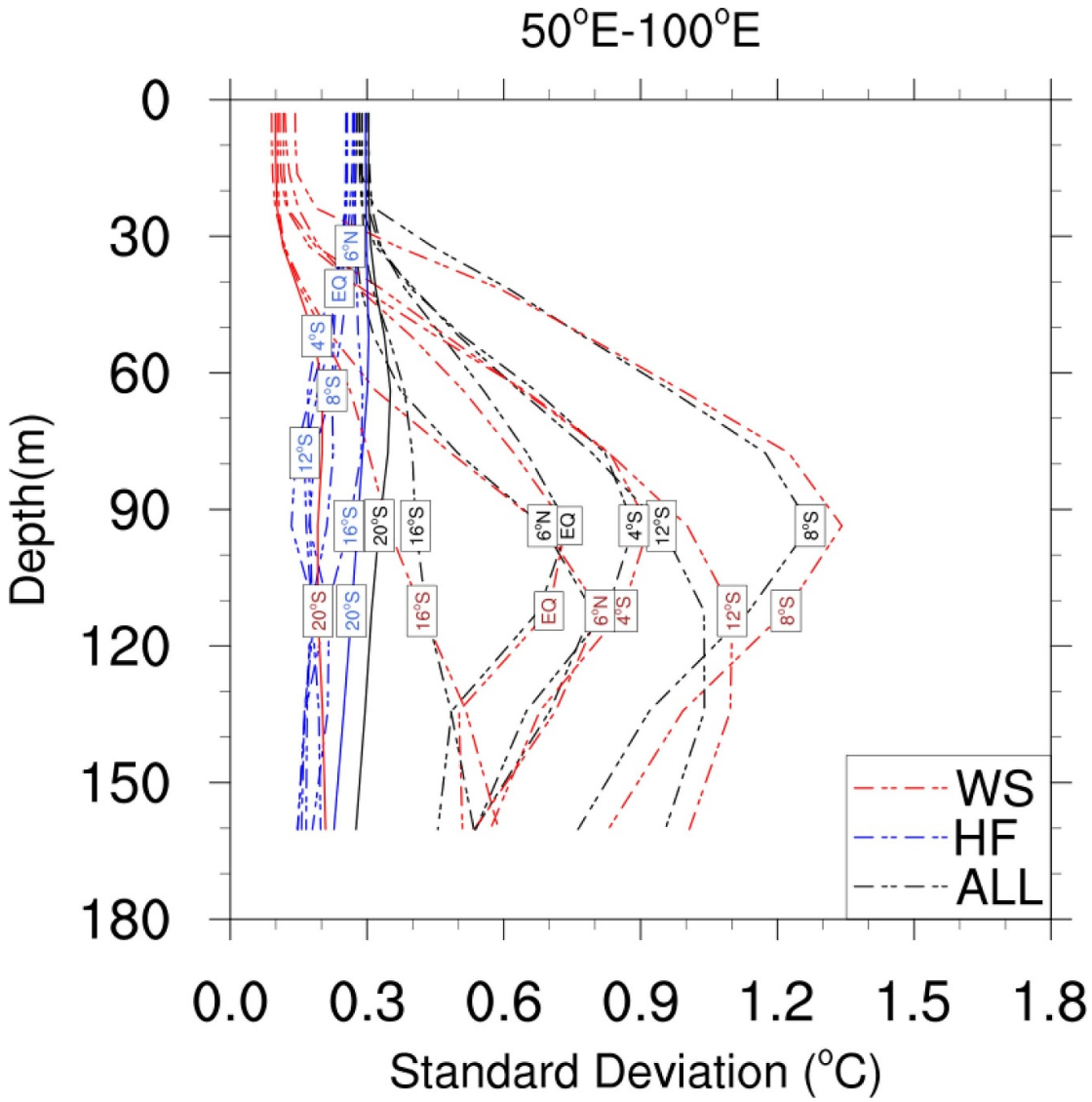

Figure 4. The profiles of the standard deviation of interannual subsurface temperature averaged along (50°E–100°E) in different latitudes versus depth. Unit:°C. Black, blue, and red lines represent ALL, HF, and WS separately. The latitudes are 6°N, equator (EQ), 4°S, 8°S, 12°S, 16°S, and 20°S, respectively.

Finally, the contributions of HF and WS to ALL in both the SCTR and the eastern part of the IOD during different seasons are shown in figure 6. The contribution of HF to ALL above the crossing depth almost reaches 100% in different seasons in both the SCTR and the eastern part of the IOD while WS contributes most to ALL below the crossing depth. It is noteworthy that wind stress almost entirely controls the interannual variability of upper-ocean temperature in the SCTR during boreal winter and spring, which is consistent with the subsurface-to-surface feedback (Xie *et al* 2002). Thicker thermocline depth in the SCTR is due to the downwelling Rossby wave and anomalous easterlies along the equatorial Indian Ocean induced by El Niño, which in turn, results in a warmer ocean surface (Xie *et al* 2002, Yokoi *et al* 2008). This strong control of wind stress leads to a shallower crossing depth in the SCTR during boreal winter and spring (figures 5(c), (d)). Shallower crossing depth can also be observed in the eastern part of the IOD during boreal winter and spring due to the dominant impact of wind stress on the interannual variability of upper-ocean temperature. But this wind stress is induced by the easterly wind anomalies (Sayantani and Gnanaseelan 2015).

4. Summary and discussion

In this study, we diagnose the relative contributions of heat flux and wind stress to the interannual upper-ocean temperature variability in the tropical Indian Ocean by analyzing three sets of high-resolution OGCM simulations that differ only in their surface forcing. ALL, forced by both interannually varying heat flux and wind stress, reasonably well reproduces the observed mean and variability of the vertical structure of ocean temperature in the tropical

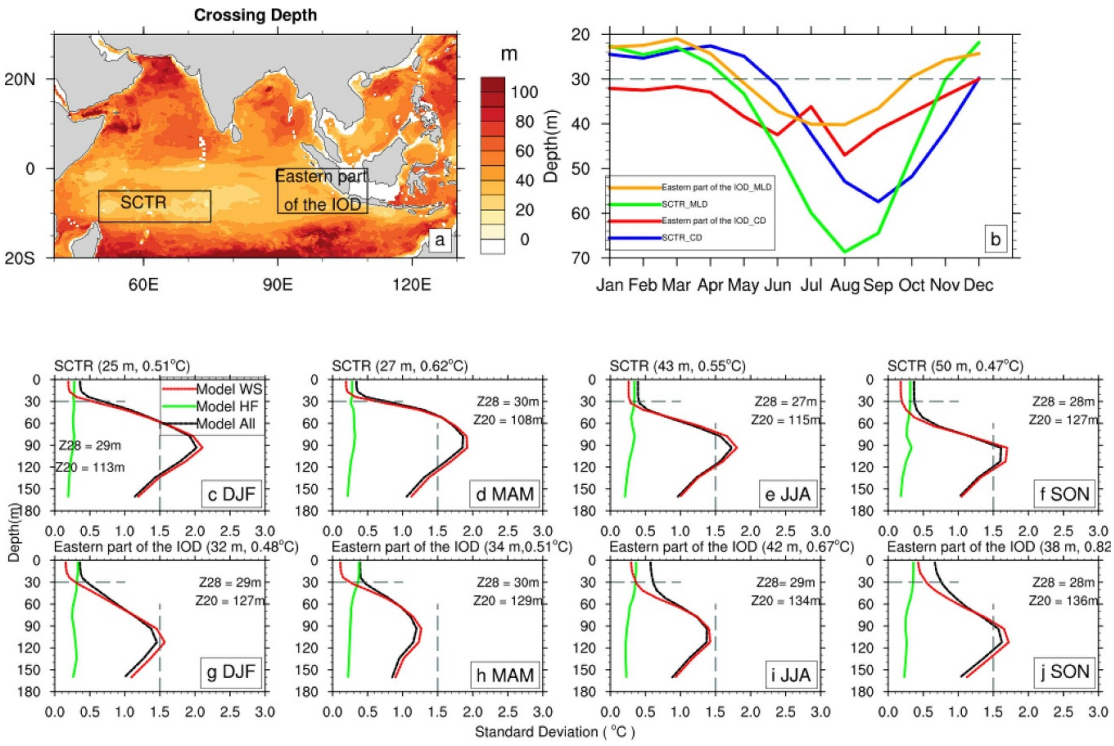

Figure 5. The distribution of the crossing depth in the tropical Indian Ocean (a) and the seasonal variations of the crossing depth and mixed layer depth (MLD) (b) and the vertical profiles of the standard deviation of interannual ocean temperature during (c), (g) DJF, (d), (h) MAM, (e), (i) JJA and (f), (j) SON averaged in the SCTR and eastern part of the IOD respectively. The boxes in (a) represent the locations of the SCTR and the eastern part of the IOD, respectively. Blue and red lines in (b) represent the crossing depth of SCTR and the eastern part of the IOD, separately. Green and orange lines in (b) represent the MLD of the SCTR and the eastern part of the IOD, respectively. Black, red and green in (c)–(j) lines represent ALL, WS, and HF, respectively. The sub-titles in (c)–(j) indicate the area, the magnitude of the crossing depth, and the standard deviation of interannual temperature responding to the crossing depth. The horizontal dashed gray line represents the depth of 30 m, and the vertical dashed line represents the 1.5 °C standard deviation. The depth of 28 °C and 20 °C isotherm, respectively, are indicated as well.

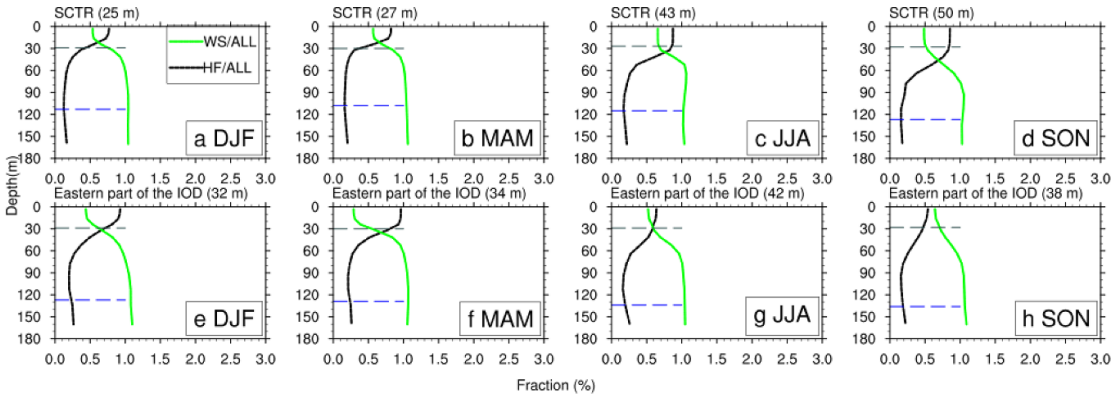

Figure 6. The vertical profiles of the contribution fraction of HF and WS to the ALL during (c), (g) DJF, (d), (h) MAM, (e), (i) JJA and (f), (j) SON averaged in the SCTR and eastern part of the IOD respectively. The horizontal dashed gray and blue lines represent the depth of the 28 °C and 20 °C isotherm, respectively.

Indian Ocean when compared to the WOA climatology and SODA reanalysis data.

Comparison of the sensitivity simulations, HF and WS, against the ALL reveals the depth-dependent impacts of heat flux and wind stress on the ocean temperature variability in the tropical Indian Ocean. In general, heat flux dominates the variability of ocean temperature in the upper 30 m in much of the tropical Indian Ocean, while its impact is quickly subdued below 30 m. On the contrary, wind stress is the decisive driver of temperature variability below 30 m. This suggests that there is a transition depth at which the main driver of the upper-ocean interannual temperature variability shifts from heat flux to wind stress. We investigated this crossing depth to better understand the driving forces of the spatial pattern and seasonality of the upper-ocean interannual temperature variability.

Our results show that the variability of ocean temperature in the top of the crossing depth is deemed mainly a response to heat flux, while the one below is induced by wind stress either locally or remotely. The shallowest crossing depth is found in the southern tropical Indian Ocean, including the SCTR and eastern part of the IOD, indicating that these are the regions where wind-stress forcing exerts a strong control on upper-ocean temperature variability. The SCTR is characterized by a shallower crossing depth along with intensified variability of the subsurface temperatures driven by wind stress, because of the anomalous wind stress and Rossby wave-induced upwelling forced by ENSO (Xie *et al* 2002, Yokoi *et al* 2012, Burns and Subrahmanyam 2016) and the Interdecadal Pacific Oscillation (Jin *et al* 2018). On the other hand, the crossing depth in the eastern part of the IOD shoals during boreal autumn and winter while it deepens in late boreal spring and summer.

The crossing depth in the SCTR also exhibits a clear seasonal variability with shoaling during boreal winter and spring and deepening during boreal summer and autumn. The strong annual cycle in the crossing depth in the SCTR is in agreement with results from previous studies (Hermes and Reason 2008, Yokoi *et al* 2008, 2009), which associated the strong annual cycle in the upper-ocean temperature in the SCTR with upwelling due to wind stress forcing related to the trade winds and Rossby waves.

Furthermore, recent high-resolution modeling studies highlight the role of ocean dynamics in setting the upper ocean temperature anomalies and variability in the tropical oceans (Roberts *et al* 2017, Small *et al* 2020). For example, Roberts *et al* (2017) adopted the Pearson correlation and a fraction of variance (FOV) skill score to diagnose the drivers of ocean variability; they showed that up to 80% of the total interannual variance of the mixed layer temperature is accounted for by the ocean heat transport convergence in the SCTR (their figure 8). We calculate the minimum vertical difference of the interannual ocean temperature standard deviation in the sensitivity experiments to distinguish the relative impacts of heat flux and wind stress. Our finding that the wind stress dominates the subsurface temperature variability in the SCTR through downwelling Rossby waves forced by wind stress, which contributes to the shoaling of the crossing depth, is consistent with their result.

Data statements

• The data that support the findings of this study are available from the corresponding author upon reasonable request.

Acknowledgments

The authors thank three anonymous reviewers for their constructive comments, which helped to substantially improve the manuscript. We also thank Erik Behrens for conducting the OGCM simulations used in this study. The integration of the OGCM simulations was performed at the North-German Supercomputing Alliance (HLRN) and the Computing Center at Kiel University. Raw model output is provided at http://data.geomar.de, and the derived fields are available upon request from the corresponding author. Comments by Claus W. Böning on an earlier version of the manuscript are gratefully acknowledged. Use of the following datasets is acknowledged: SODA (http://sodaserver.tamu.edu/assim/) and WOA09 (www.nodc.noaa.gov/OC5/WOA09/pr_woa09.html). This research was supported by a Research Fellowship by the Alexander von Humboldt Foundation to CCU. HS is grateful for support by ONR (N00014-17-1-2398) and NOAA (NA17OAR4310255).

ORCID iDs

Xu Yuan https://orcid.org/0000-0002-4612-7344
Caroline C Ummenhofer https://orcid.org/0000-0002-9163-3967

References

Alexander M A, Bladé I, Newman M, Lanzante J R, Lau N-C and Scott J D 2002 The atmospheric bridge: the influence of ENSO teleconnections on air–sea interaction over the global oceans *J. Clim.* **15** 2205–31

Annamalai H, Liu P and Xie S-P 2005 Southwest Indian Ocean SST variability: its local effect and remote influence on Asian monsoons *J. Clim.* **18** 4150–67

Ashok K, Guan Z, Saji N and Yamagata T 2004 Individual and combined influences of ENSO and the Indian Ocean dipole on the Indian summer monsoon *J. Clim.* **17** 3141–55

Baquero-Bernal A, Latif M and Legutke S 2002 On dipolelike variability of sea surface temperature in the tropical Indian Ocean *J. Clim.* **15** 1358–68

Behera S, Salvekar P and Yamagata T 2000 Simulation of interannual SST variability in the tropical Indian Ocean *J. Clim.* **13** 3487–99

Behera S K and Yamagata T 2001 Subtropical SST dipole events in the southern Indian Ocean *Geophys. Res. Lett.* **28** 327–30

Behrens E, Biastoch A and Böning C W 2013 Spurious AMOC trends in global ocean sea-ice models related to subarctic freshwater forcing *Ocean Model.* **69** 39–49

Bernard B, Madec G, Penduff T, Molines J-M, Treguier A-M, Le Sommer J, Beckmann A, Biastoch A, Böning C and Dengg J 2006 Impact of partial steps and momentum advection schemes in a global ocean circulation model at eddy-permitting resolution *Ocean Dyn.* **56** 543–67

Blanke B and Delecluse P 1993 Variability of the tropical Atlantic Ocean simulated by a general circulation model with two different mixed-layer physics *J. Phys. Oceanogr.* **23** 1363–88

Burns J M and Subrahmanyam B 2016 Variability of the seychelles–chagos thermocline ridge dynamics in

connection with ENSO and Indian Ocean Dipole *IEEE Geosci. Remote. Sens. Lett.* **13** 2019–23
Chen G, Han W, Li Y and Wang D 2016 Interannual variability of equatorial eastern Indian Ocean upwelling: local versus remote forcing *J. Phys. Oceanogr.* **46** 789–807
Cyriac A, Mcphaden M, Phillips H, Bindoff N and Feng M 2019 Seasonal evolution of the surface layer heat balance in the eastern subtropical Indian Ocean *J. Geophys. Res. Oceans* **124** 6459–77
Delman A S, Sprintall J, Mcclean J L and Talley L D 2016 Anomalous Java cooling at the initiation of positive Indian Ocean Dipole events *J. Geophys. Res. Oceans* **121** 5805–24
Du Y, Xie S-P, Huang G and Hu K 2009 Role of air–sea interaction in the long persistence of El Niño–induced north Indian Ocean warming *J. Clim.* **22** 2023–38
Fichefet T and Maqueda M A M 1997 Sensitivity of a global sea ice model to the treatment of ice thermodynamics and dynamics *J. Geophys. Res.* **102** 12609–46
Griffies S M, Biastoch A, Böning C, Bryan F, Danabasoglu G, Chassignet E P, England M H, Gerdes R, Haak H and Hallberg R W 2009 Coordinated ocean-ice reference experiments (COREs) *Ocean Model.* **26** 1–46
Han W, Vialard J, Mcphaden M J, Lee T, Masumoto Y, Feng M and De Ruijter W P 2014 Indian Ocean decadal variability: a review *Bull. Am. Meteorol. Soc.* **95** 1679–703
Hermes J and Reason C 2008 Annual cycle of the South Indian Ocean (Seychelles-Chagos) thermocline ridge in a regional ocean model *J. Geophys. Res. Oceans* **113** C04035
Huang B and Kinter J L III 2002 Interannual variability in the tropical Indian Ocean *J. Geophys. Res. Oceans* **107** 20-21–20-26
Jin X, Kwon Y-O, Ummenhofer C C, Seo H, Schwarzkopf F U, Biastoch A, Böning C W and Wright J S 2018 Influences of Pacific climate variability on decadal subsurface ocean heat content variations in the Indian Ocean *J. Clim.* **31** 4157–74
Klein S A, Soden B J and Lau N-C 1999 Remote sea surface temperature variations during ENSO: evidence for a tropical atmospheric bridge *J. Clim.* **12** 917–32
Large W G and Yeager S 2009 The global climatology of an interannually varying air–sea flux data set *Clim. Dyn.* **33** 341–64
Lau N-C and Nath M J 2003 Atmosphere–ocean variations in the Indo-Pacific sector during ENSO episodes *J. Clim.* **16** 3–20
Levitus S *et al* 1998 World Ocean Database 1998 volume 1: Introduction NOAA Atlas *NESDIS* **18** 346
Levitus S *et al* 2012 World ocean heat content and thermosteric sea level change (0–2000 m), 1955–2010 *Geophys. Res. Lett.* **39** L10603
Levitus S, Antonov J I, Boyer T P, Locarnini R A, Garcia H E and Mishonov A V 2009 Global ocean heat content 1955–2008 in light of recently revealed instrumentation problems *Geophys. Res. Lett.* **36** L07608
Liu Z and Alexander M 2007 Atmospheric bridge, oceanic tunnel, and global climatic teleconnections *Rev. Geophys.* **45** RG2005
Madec G 2008 NEMO ocean engine, version 3.1. L'Institut Pierre-Simon Laplace *Tech. Rep.* **27** 27
Moisan J R and Niiler P P 1998 The seasonal heat budget of the North Pacific: net heat flux and heat storage rates (1950–1990) *J. Phys. Oceanogr.* **28** 401–21
Murtugudde R and Busalacchi A J 1999 Interannual variability of the dynamics and thermodynamics of the tropical Indian Ocean *J. Clim.* **12** 2300–26
Nagura M and Konda M 2007 The seasonal development of an SST anomaly in the Indian Ocean and its relationship to ENSO *J. Clim.* **20** 38–52
Qu T and Meyers G 2005 Seasonal variation of barrier layer in the southeastern tropical Indian Ocean *J. Geophys. Res. Oceans* **110** C11003
Rao R and Sivakumar R 2000 Seasonal variability of near-surface thermal structure and heat budget of the mixed layer of the tropical Indian Ocean from a new global ocean temperature climatology *J. Geophys. Res. Oceans* **105** 995–1015
Rao S A and Behera S K 2005 Subsurface influence on SST in the tropical Indian Ocean: structure and interannual variability *Dyn. Atmos. Oceans* **39** 103–35
Roberts C D, Palmer M D, Allan R P, Desbruyeres D G, Hyder P, Liu C and Smith D 2017 Surface flux and ocean heat transport convergence contributions to seasonal and interannual variations of ocean heat content *J. Geophys. Res. Oceans* **122** 726–44
Saji N, Goswami B N, Vinayachandran P and Yamagata T 1999 A dipole mode in the tropical Indian Ocean *Nature* **401** 360–3
Sayantani O and Gnanaseelan C 2015 Tropical Indian Ocean subsurface temperature variability and the forcing mechanisms *Clim. Dyn.* **44** 2447–62
Schott F A, Xie S P and Mccreary J P 2009 Indian Ocean circulation and climate variability *Rev. Geophys.* **47** RG1002
Schwarzkopf F U and Böning C W 2011 Contribution of Pacific wind stress to multi-decadal variations in upper-ocean heat content and sea level in the tropical south Indian Ocean *Geophys. Res. Lett.* **38** L12602
Shinoda T, Alexander M A and Hendon H H 2004a Remote response of the Indian Ocean to interannual SST variations in the tropical Pacific *J. Clim.* **17** 362–72
Shinoda T, Hendon H H and Alexander M A 2004b Surface and subsurface dipole variability in the Indian Ocean and its relation with ENSO *Deep Sea Res. Part I: Oceanogr. Res. Pap.* **51** 619–35
Singh P, Chowdary J S and Gnanaseelan C 2013 Impact of prolonged La Niña events on the Indian Ocean with a special emphasis on southwest tropical Indian Ocean SST *Glob. Planet. Change* **100** 28–37
Small R J, Bryan F O, Bishop S P, Larson S and Tomas R A 2020 What drives upper-ocean temperature variability in coupled climate models and observations? *J. Clim.* **33** 577–96
Tanizaki C, Tozuka T, Doi T and Yamagata T 2017 Relative importance of the processes contributing to the development of SST anomalies in the eastern pole of the Indian Ocean Dipole and its implication for predictability *Clim. Dyn.* **49** 1289–304
Trenary L L and Han W 2012 Intraseasonal-to-interannual variability of South Indian Ocean sea level and thermocline: remote versus local forcing *J. Phys. Oceanogr.* **42** 602–27
Ummenhofer C C, Biastoch A and Böning C W 2017 Multi-decadal Indian Ocean variability linked to the Pacific and implications for preconditioning Indian Ocean dipole events *J. Clim.* **30** 1739–51
Ummenhofer C C, Schwarzkopf F U, Meyers G, Behrens E, Biastoch A and Böning C W 2013 Pacific Ocean contribution to the asymmetry in eastern Indian Ocean variability *J. Clim.* **26** 1152–71
Vialard J, Duvel J-P, Mcphaden M J, Bouruet-Aubertot P, Ward B, Key E, Bourras D, Weller R, Minnett P and Weill A 2009 Cirene: air—sea interactions in the Seychelles—Chagos thermocline ridge region *Bull. Am. Meteorol. Soc.* **90** 45–62
Wu R, Kirtman B P and Krishnamurthy V 2008 An asymmetric mode of tropical Indian Ocean rainfall variability inboreal spring *J. Geophys. Res.* **113** D05104
Xie S-P, Annamalai H, Schott F A and Mccreary J P Jr 2002 Structure and mechanisms of South Indian Ocean climate variability *J. Clim.* **15** 864–78
Yamagata T, Behera S K, Luo -J-J, Masson S, Jury M R and Rao S A 2004 Coupled ocean-atmosphere variability in the tropical Indian Ocean *Earth's Clim.: Ocean–Atmosp. Interact. Geophys. Monogr.* **147** 189–212
Yokoi T, Tozuka T and Yamagata T 2008 Seasonal variation of the Seychelles Dome *J. Clim.* **21** 3740–54
Yokoi T, Tozuka T and Yamagata T 2009 Seasonal variations of the Seychelles Dome simulated in the CMIP3 models *J. Phys. Oceanogr.* **39** 449–57
Yokoi T, Tozuka T and Yamagata T 2012 Seasonal and interannual variations of the SST above the Seychelles Dome *J. Clim.* **25** 800–14

Yu L, Jin X and Weller R A 2007 Annual, seasonal, and interannual variability of air–sea heat fluxes in the Indian Ocean *J. Clim.* **20** 3190–209

Yu W, Xiang B, Liu L and Liu N 2005 Understanding the origins of interannual thermocline variations in the tropical Indian Ocean *Geophys. Res. Lett.* **32** L24706

Yuan X, Salama M and Su Z 2018 An observational perspective of sea surface salinity in the Southwestern Indian Ocean and its role in the South Asia Summer Monsoon *Remote Sens.* **10** 1930

Zhong A, Hendon H H and Alves O 2005 Indian Ocean variability and its association with ENSO in a global coupled model *J. Clim.* **18** 3634–49

Zhou L, Murtugudde R and Jochum M 2008 Seasonal influence of Indonesian throughflow in the southwestern Indian Ocean *J. Phys. Oceanogr.* **38** 1529–41